Turkish Journal of Electrical Engineering & Computer Sciences

http://journals.tubitak.gov.tr/elektrik/

Research Article

Turk J Elec Eng & Comp Sci
(2022) 30: 2179 – 2189

doi:10.55730/1300-0632.3932

A compact pattern reconfigurable antenna employing shorted quarterwave patch antennas

Feza Turgay ÇELİK*, **Lale ALATAN**, **Özlem AYDIN ÇİVİ**
Department of Electrical and Electronics Engineering, Faculty of Engineering, Middle East Technical University, Ankara, Turkey

Received: 31.01.2022 • **Accepted/Published Online:** 02.06.2022 • **Final Version:** 28.09.2022

Abstract: In this study, a compact pattern reconfigurable antenna structure is proposed. The proposed antenna is a half-wave square microstrip patch antenna divided into two quarter-wave antenna portions by a conducting wall. This wall forces potential zero at the connection point; therefore, it separates the antenna into two independent quarter-wave portions. Pattern reconfiguration is achieved by separate feeding of the quarter-wave portions. Phase difference between excitations of antenna ports result in variation at the maximum beam direction. Hence, pattern reconfiguration is achieved. Within such a compact antenna, beam steering up to 40^0 is achieved.

Key words: Reconfigurable antenna, antenna design, beam steering, conical beam, shorted patch

1. Introduction

Increased demand for higher data rates and increased capacity in modern communication systems requires the design of sophisticated antenna structures. This demand in 5G protocol applications like multi-input-multi-output (MIMO) systems can be achieved by utilizing spatial diversity through pattern reconfigurable antenna structures. In the last decade, a vast number of pattern reconfigurable antennas have been studied to address this problem. The techniques employed to obtain different radiation patterns from a radiating structure can be divided into several categories. The first category employs parasitic radiators to change the orientation of the radiation pattern [1, 2]. In these studies, parasitic elements having different sizes are placed in the immediate vicinity of the main radiating structure. Controlling the size of the parasitic elements yields a tilt in the radiation pattern towards or away from the parasitic element. Another approach to reshaping the radiation pattern could be shorting parasitic elements instead of changing their sizes as in [2].

In the second class of pattern reconfigurable antennas, different radiators are combined to form a single antenna [3–5]. In these studies, generally, antennas with broadside radiation and conical patterns are combined. For example in [3] an annular ring and a circular patch antenna are placed concentrically. The sizes of the ring and circular patch are designed to operate the circular patch at TM_{11} mode and the ring at TM_{21} mode. By designing a switchable feed network appropriate for the excitation of each mode, broadside (TM_{11} mode) or conical (TM_{21} mode) radiation characteristics can be obtained. In [4], a printed dipole with a director and a printed monopole are combined to achieve a broadside beam by exciting the former radiator and a conical beam by exciting the latter one. A wideband pattern reconfigurable antenna that can switch between dipole

*Correspondence: feza.celik@metu.edu.tr

radiation mode and endfire (left/right) radiation modes is proposed in [5] by utilizing the slot between two arms of a wide dipole antenna as a Vivaldi antenna. As the size of such combined radiator type antennas and parasitic element employing antennas are large, they are not suitable for large-scale array applications like massive MIMO systems.

The third class of pattern reconfigurable antennas suggests the excitation of different modes of a single radiator [6, 7]. The fundamental and higher-order modes have different radiation characteristics. For example, the rectangular patch antenna illustrates a broadside radiation pattern in TM_{01} mode, while it produces a conical beam at TM_{02} mode [6]. However, since resonance frequencies of two different modes are also different, complicated matching circuits and/or inclusion of tuning components into the antenna structure are required to obtain different radiation patterns at the same frequency. Therefore, these antennas are also not good candidates for massive MIMO applications.

The fourth class of pattern reconfigurable antennas divide a single radiator into subregions by using shorting vias or shorting plates. Excitation of each radiator with different phase and/or amplitude provides pattern reconfiguration. For example, in [8] a half-wavelength rectangular patch is divided into two quarter-wave short-circuited patches by utilizing a shorting plate at the center. The in-phase and out-of-phase excitation of these two sub-radiators results in conical and broadside beams, respectively. In [8], these two operation modes are obtained through two input ports of a 180^0 rat-race coupler whose output ports are used to excite two subradiators by aperture coupling. Moreover, a null in the radiation pattern is steered by exciting the input ports of the coupler with different amplitudes. In [9], a square patch antenna is divided into four triangular subradiators by using shorting vias at the corners. This planar structure provides beam scanning in two dimensions by exciting each subradiator with different phase and magnitude combinations.

This study aims to design a compact pattern reconfigurable antenna suitable for large array applications. The antenna structure proposed in [8] is modified to avoid the use of the 180^0 rat-race coupler that limits the bandwidth of the antenna (3.5%). Moreover, the feed structure is also simplified to make it more compatible with a large array application requirements. As a result, as first proposed in our previous work [10], the feed structure is chosen to be coaxial feed and the two ports of the antenna are directly combined through a phase shifter. By eliminating the use of rat-race coupler, an antenna with wider bandwidth (5.5%) is obtained even though a thinner ($0.018\lambda_0$) substrate with a higher dielectric constant ($\epsilon_r = 2.2$) is used, compared to the antenna in [8], build with $0.053\lambda_0$ thick air substrate. By employing various phase values between the two ports of the antenna it is demonstrated that the main radiation direction of the antenna can be steered between -40^0 and $+40^0$ in the elevation plane. In this study, a reconfigurable antenna that can steer its beam in one plane is considered since it is aimed to be used in a linear array. If 2D beam steering is required, planar structures with four subradiators as in [9] should be studied.

In Section 2, the proposed structure is introduced together with the studied parameters, and the radiation mechanism of the antenna is summarized. The even/odd mode concept is introduced and the effects of different combinations of modes on the radiation characteristics of the antenna are explained through demonstrative examples in Section 3. In Section 4, simulation results obtained by a commercially available electromagnetic field simulator (ANSYS HFSS) and measurement results of the fabricated prototype are presented and compared. Conclusions follow this section.

2. Antenna structure

The proposed antenna is designed for the sub-6 GHz region of the European Zone 5G applications; therefore, 3.6 GHz is selected as an operating frequency. In the microstrip structure, Rogers 5880 dielectric plate ($\epsilon_r = 2.2, tan\delta = 0.0009$) with 1.524 mm thickness is used as a substrate. The square patch antenna is divided into two quarter-wave antennas by shorting plate, as shown in Figure 1a. This connection separates the antenna into two independent subradiators. These radiators are excited with different SMA connectors located d apart from the shorting plate. For a better understanding of the independent excitation of the half patches, side view of the antenna is provided in Figure 1b. Dimensions illustrated in Figure 1a can be found in Table 1.

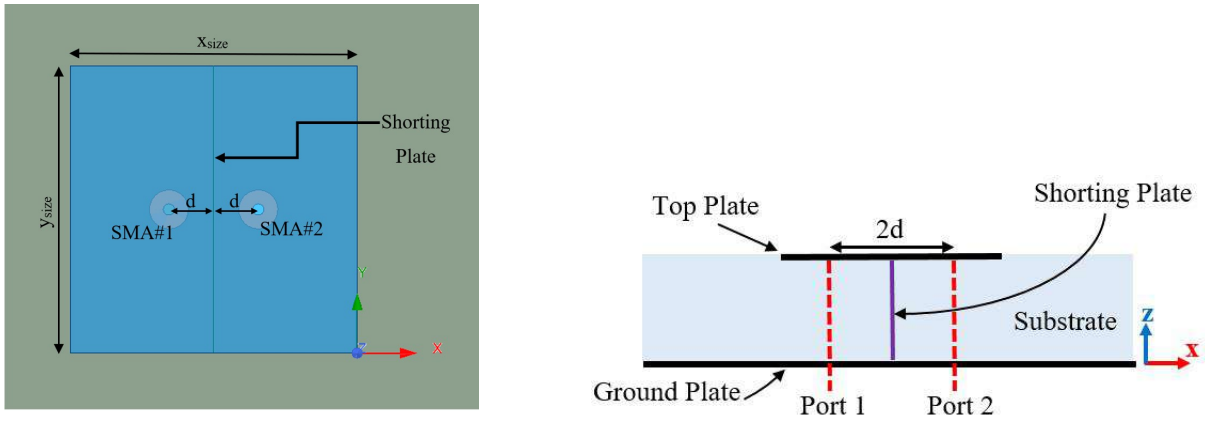

(a) (b)

Figure 1. Top (a) and side (b) view of the antenna.

Table 1. Dimensions of the antenna.

Dimension	Value in mm
x_{size}	25.7
y_{size}	25.7
d	4
Substrate size	100 x 100

To determine the X_{size} of the antenna, first, an initial point is chosen as $\lambda_g/2 = 27.4$ mm by calculating the guided wavelength through empirical formulas in [11]. Then parametric sweep is performed in ANSYS HFSS to fine-tune this parameter and reach X_{size}=25.7 mm. Similarly, the d parameter of the antenna is also optimized by using the parametric analysis tool of HFSS. To excite the antenna, standard SMA connectors having a diameter of 4.13 mm are preferred.

Distinct radiation beam shapes of the antenna can be understood by inspecting even and odd modes concept in rectangular patch structures. This analysis is also used in [8] for the same purpose. As mentioned before, the existence of shorting plane enables two independent excitations for the antenna. The phase difference between excitations determines the E-field distribution and equivalent magnetic currents at the radiating edges which stem from these E-fields. Even mode represents the case where excitations are out of phase, while odd mode occurs when quarter-wave portions are excited in phase. The E-field distributions and equivalent magnetic currents at the radiating edges ($\vec{M}$) can be seen in Figure 2.

(a) (b)

Figure 2. E-field and magnetic current distributions for (a) even and (b) odd modes.

Mode naming is done regarding the directions of the radiating magnetic currents. When these currents are in the same direction, antenna operates in even mode as in Figure 2a, likewise when the currents are in opposite directions antenna operates in odd mode as seen in Figure 2b. The radiated fields by magnetic currents represented in even mode superposed constructively in a broadside direction. Therefore, the main beam is in the broadside direction. On the other hand, the radiated fields by odd mode operation cancel out in the broadside direction. So, the radiation is directed to a higher scan angle in the θ direction. This type of radiated beam is called a conical beam or monopole-like beam. The radiated fields of even and odd modes of operations can be seen in Figures 3a and Figure 3b respectively.

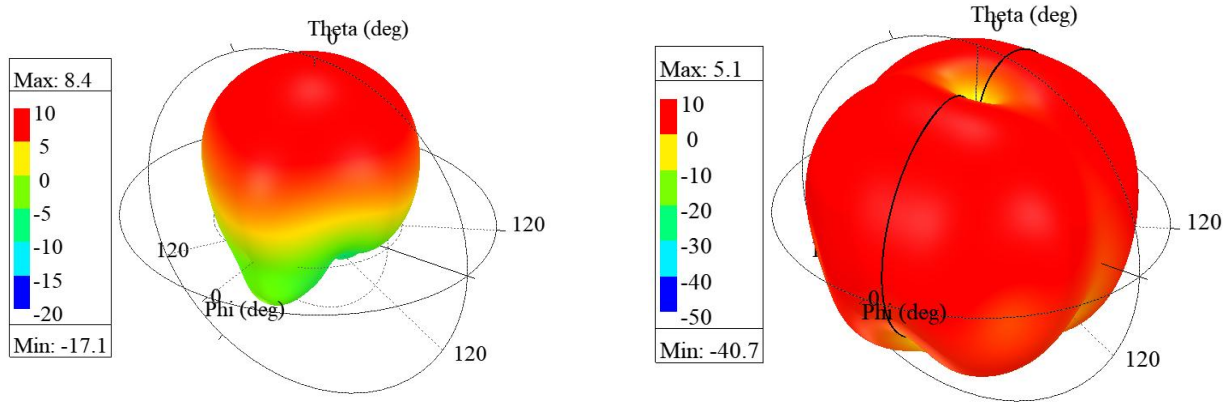

(a) (b)

Figure 3. Directivity patterns of (a) even and (b) odd mode of operation in rectangular patch antenna in 3D [dB].

3. Operation principle and beam scanning

The antenna is designed to operate with beam scanning ability; therefore, operating with only even and odd modes is insufficient. In order to cover $[-40^0; +40^0]$ range in elevation (θ), different combinations of the even and odd modes are necessary. A combination of even and odd modes in different ratios is conducted by applying the intermediate phase difference between excitations.

As illustrated before, out-of-phase excitation ($\beta = 180^0$) of ports yields a broadside beam while in-phase excitation ($\beta = 0^0$) yields a conical beam. When a different phase difference is applied, the radiation pattern shifts from these patterns. For instance, if the phase difference between excitations (β) is selected as 30^0, the maximum radiation direction is observed to be in the $\theta = -30^0$ direction. As the amount of phase difference is closer to the in-phase case, the effect of the odd mode is more pronounced than the even mode. The opposite can be observed when the phase difference between excitations is 120^0. In this case, the effect of the even mode is more dominant compared to the odd mode as the phase difference between ports is closer to 180^0. So a lower elevation angle is scanned.

The effect of the different phase combinations also can be understood by inspecting surface current distributions under different feeding combinations. Surface currents on the rectangular patch can be seen in Figure 4.

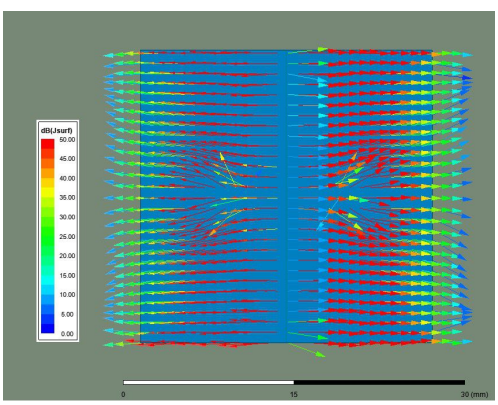

(a) $\beta = 0^0$

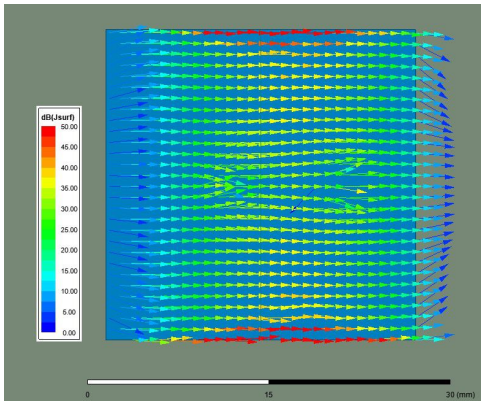

(b) $\beta = 180^0$

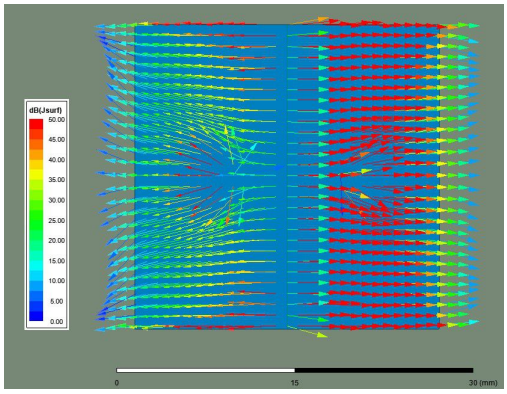

(c) $\beta = 30^0$

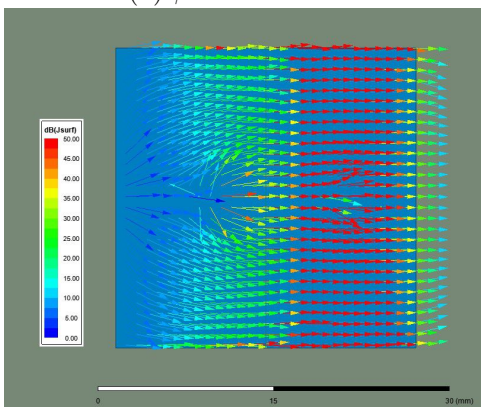

(d) $\beta = 90^0$

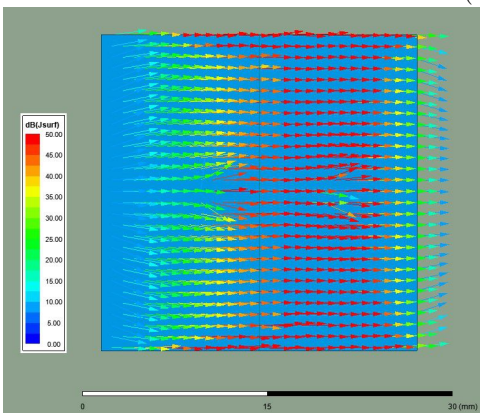

(e) $\beta = 120^0$

Figure 4. Surface current distributions when different phase differences between ports are applied (from a-e: $\beta = 0^0, 180^0, 30^0, 90^0, 120^0$).

When $\beta = 0^0$ is applied to the patches, there exists a current null line in the merging line of the patches as seen in Figure 4a. This null results in surface currents that are directed in opposite directions, yielding a

conical beam. On the other hand, when $\beta = 180^0$ is applied, only one dominant current flows through the whole patch as seen in Figure 4b. As there are no opposing currents, broadside radiation is observed at the $\beta = 180^0$ case. The current distributions of intermediate phase differences are formed by the superposition of $\beta = 0^0$ and $\beta = 180^0$ cases in different ratios. Differences in current distributions and dominance of the modes can be seen in Figures 4c–4e. The list of radiated beam directions with respect to different excitation combinations can be seen in Table 2.

Table 2. The direction of main beams at $\phi = 0^0$ plane when different phase combinations are applied from Port 1 and Port 2 ports.

Applied phase from Port1	Applied phase from Port2	Main beam direction at $\phi = 0^0$ plane
0^0	0^0	$\theta = \pm 40^0$
30^0	0^0	$\theta = -30^0$
90^0	0^0	$\theta = -23^0$
120^0	0^0	$\theta = -13^0$
0^0	30^0	$\theta = 30^0$
0^0	90^0	$\theta = 23^0$
0^0	120^0	$\theta = 13^0$
180^0	0^0	$\theta = 0^0$

The applied phase notation in Table 2 corresponds to the delay phenomena. For example, the second row of the table represents the case when Port 1 lags behind Port 2 excitation with a 30^0 difference. The illustration of several radiation patterns can be seen in Figure 5. It is observed from Figure 5 and Table 2 that $\pm 40^0$ beam rotation can be achieved with the proposed antenna. Note that radiation patterns remain the same in the operational bandwidth.

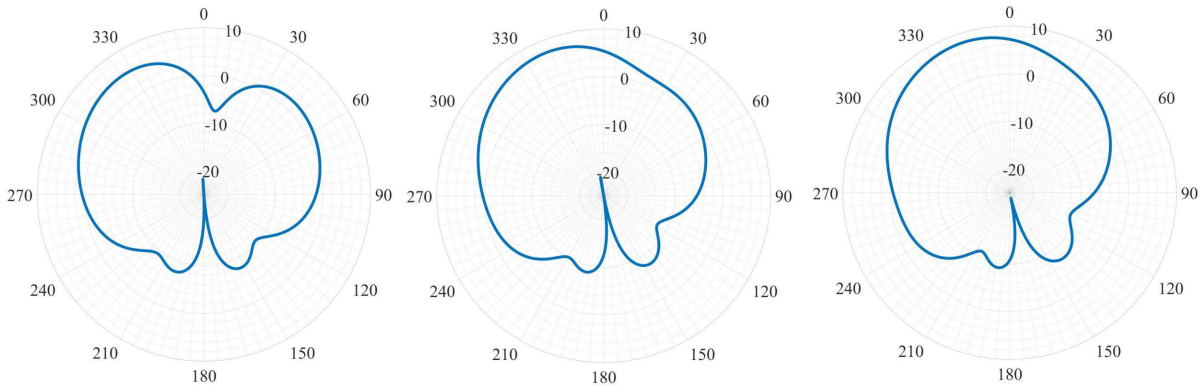

Figure 5. Simulated normalized gain patterns at $\phi = 0^0$ plane of the patch antenna when different phase differences ($\beta = 30^0, 90^0, 120^0$) are applied between ports. (a), (b), (c).

4. Measurement results

A prototype of the designed antenna is fabricated to validate the beam steering performance. Rogers 5880 laminate with 1.524 mm thickness and loss tangent of 0.0009 is milled to fabricate the antenna. The top view of the fabricated prototype can be seen in Figure 6.

Figure 6. Top view of the prototype antenna.

Measured S_{11} values as a function of frequency are plotted and compared with simulation results in Figure 7. As seen, the antenna resonates at 3.6 GHz and it is in agreement with measurement results. The antenna has a symmetric feed structure; therefore, it is expected to have similar $|S_{11}|$ and $|S_{22}|$ behavior. Measurements of these S-parameters are illustrated in Figure 7 which demonstrates that the characteristic of $|S_{11}|$ and $|S_{22}|$ parameters are the same.

The S_{11} behavior of the prototype antenna has a more broadband characteristic compared to the simulated one. This difference can be explained by the excess losses of the fabricated antenna. The excess solder material and the connection points of the conducting wall at the middle section of the antenna seen in Figure 6 introduce additional losses. In addition to S_{11}, the S_{21} parameters of the antenna are also measured. The comparative illustration of the measurement and simulation results of the S-parameters can be seen in Figures 7 and 8.

The magnitude of S_{21} value of the antenna in the interest frequency is measured as –6.5 dB. This relatively high S_{21} value might be due to the surface wave coupling through the common dielectric substrate and ground plane also due to the space wave coupling between patches. To improve the isolation of the antenna, the shorting plate is extended above the patches and also to the sides of the dielectric substrate. Although the isolation is reduced to –15 dB at the operating frequency according to simulation results, slight improvement in the gain of the antenna is observed. Since the two ports will be combined and the final antenna will be a one-port device, the isolation between the ports is not evaluated to be an improvement performance parameter for this application.

Radiation patterns for phase differences of $\beta = 0^0, 30^0, 90^0, 120^0, 180^0$ cases are measured in the anechoic chamber. The measured radiation patterns are plotted and compared with simulated ones in Figure 9. The measurement results are in excellent agreement with the simulated ones. Also, they demonstrate the beam steering ability of the antenna element. There are some fluctuations and ripples in the measurements at

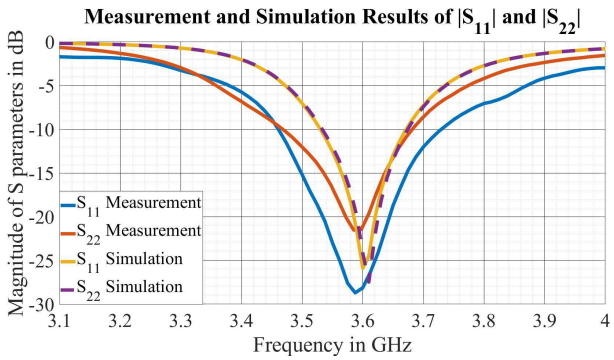

Figure 7. Measurement and simulation results of the S_{11} parameter.

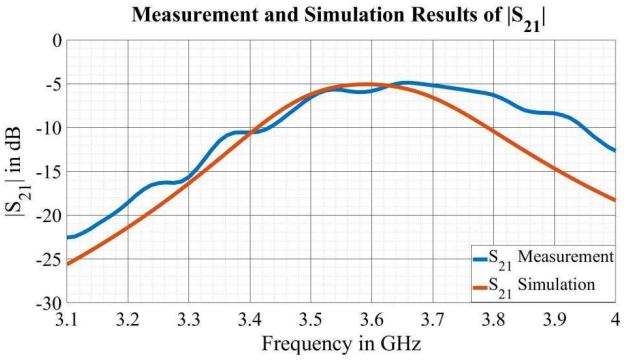

Figure 8. Measurement and simulation results of the S_{21} parameter.

$\beta = 30^0$ and $\beta = 90^0$ cases. These ripples occur due to minor physical vibrations at the measurement setup. The radiation pattern measurements prove the beam steering performance of the antenna within -40^0 to $+40^0$ in the elevation plane. The measured main beam directions and the simulated ones can be compared from Table 3. The measurement results of the antenna also proves the beam scanning performance of the antenna in $\pm 40^0$ interval.

In addition to the S_{11} and radiation pattern measurements, the gain of the antenna at different steering angles are measured. The gain measurements are taken only at the resonance frequency of 3.6 GHz. The gain values and their comparison are listed in Table 4. The simulated and measured maximum gains of the antenna illustrate remarkable resemblance.

To highlight the performance of the proposed antenna compared to the ones in the literature, a comparison table is provided in Table 5. Note that, since the antennas will be used in an array configuration, only patch or dipole size is considered in lateral dimensions. As it can be seen from this table, the proposed antenna achieves reasonable frequency bandwidth with a compact size and low profile. The proposed antenna achieves a wider bandwidth with smaller electrical size compared to the antennas reported in [8] and [9]. The antennas proposed in [4] and [7] provide wider bandwidth with a cost of increased electrical size. The large electrical size of the radiators in [4] and [7] limit their use in scanning array applications. In addition to that, the end-fire radiation characteristics of the antenna proposed in [4] does not allow its use in planar array applications. As a result, only the proposed antenna is suitable for beam scanning planar array applications due to its electrical size of less than half wavelength.

Table 3. Measurement and simulation results of the main beam direction and simulated maximum gain values under different excitation cases (at $\phi = 0^0$ plane).

Phase difference between ports	Simulated main beam direction	Measured main beam direction	Simulated maximum gain
0^0	$\theta = \pm 40^0$	$\theta = \pm 40^0$	3.85 dB
30^0	$\theta = 30^0$	$\theta = 28^0$	5.2 dB
90^0	$\theta = 23^0$	$\theta = 23^0$	7.34 dB
120^0	$\theta = 13^0$	$\theta = 14^0$	7.95 dB
180^0	$\theta = 0^0$	$\theta = 0^0$	8.53 dB

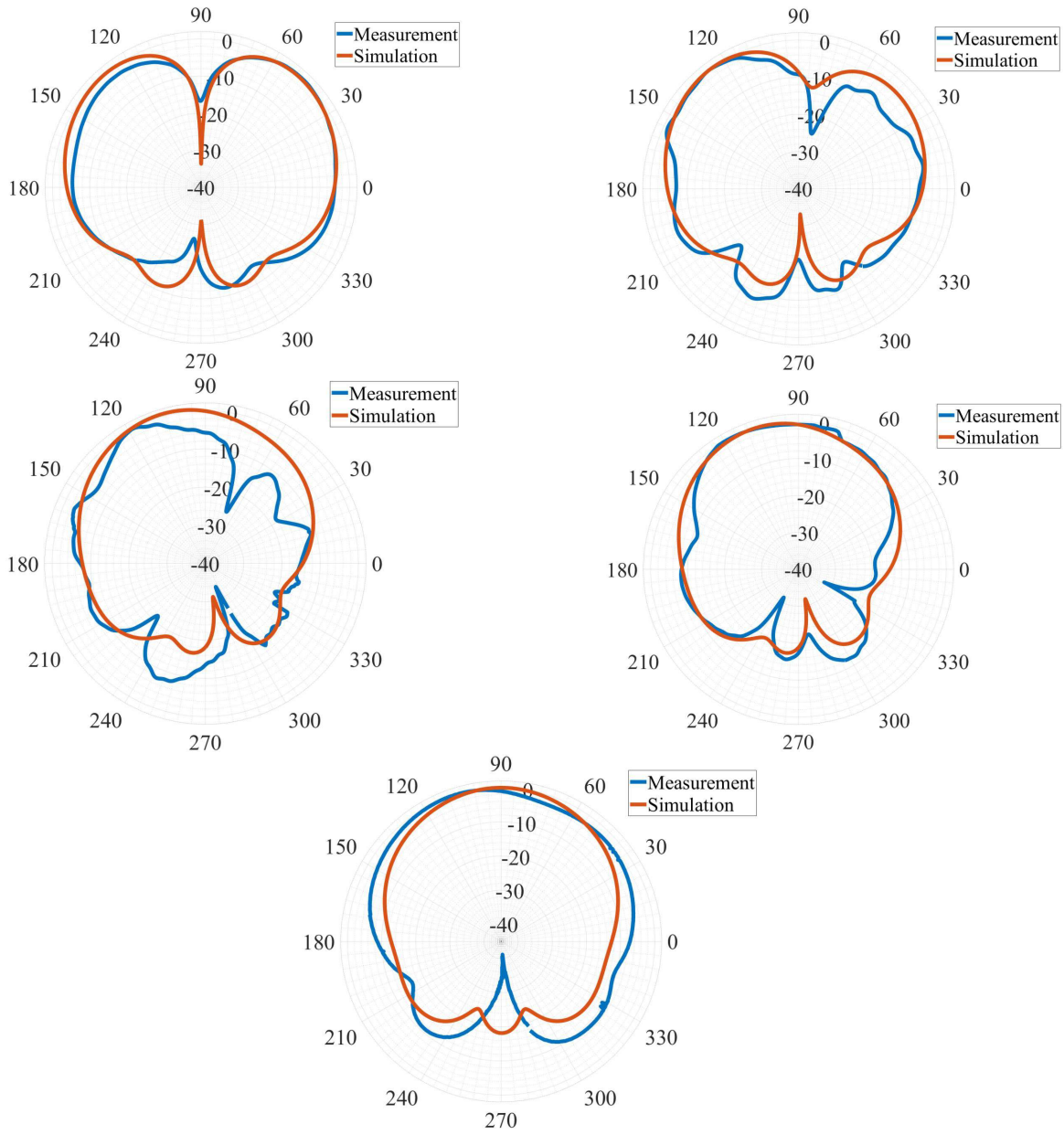

Figure 9. Compared radiation patterns for $\beta = 0^0, 30^0, 90^0, 120^0, 180^0$ at $\phi = 0^0$ plane.

Table 4. Measured and simulated gain values of the antenna.

	Max. gain in broadside beam ($\beta = 180^0$) [dB]	Max. gain in conical beam ($\beta = 0^0$) [dB]
Simulation	8.53	3.85
Measurement	8.48	3.83

5. Conclusion

In this article, a compact pattern reconfigurable square patch antenna which is divided into two quarterwave patches with a shorting plate is proposed as a good candidate for MIMO array applications. These quarterwave

Table 5. Comparison with similar studies in the literature.

Study	Freq. (GHz)	Antenna substrate	Size/$(\lambda_0)^3$	BW (%)	Feeding technique
[4]	3	FR4 ($\epsilon_r = 4.4$)	$0.511 \times 0.244 \times 0.005$	14.1	CPW and microstrip line feed combination
[7]	2.5	FR4 ($\epsilon_r = 4.4$)	$0.73 \times 0.73 \times 0.12$	7.8	Proximity coupled feeding with multiple ports
[8]	2.45	Air	$0.41 \times 0.37 \times 0.053$	3.5	Aperture coupled two ports combined with a Rat-Race coupler.
[9]	2.4	TLP5 ($\epsilon_r = 2.2$)	$0.61 \times 0.61 \times 0.012$	1.7	Coaxial probe feed
Proposed antenna	3.6	Rogers 5880 ($\epsilon_r = 2.2$)	$0.3 \times 0.3 \times 0.018$	5.5	Coaxial probe feed

patches are excited separately by the same amplitude with a phase difference to rotate the beam. Out of phase excitation results in broadside radiation whereas in-phase excitation gives conical radiation pattern. It is shown that by applying different phase combinations, beam can be rotated to the directions in between. Measured radiation patterns of the fabricated antenna agree very well with the simulations. It is demonstrated that the maximum radiation direction of the antenna can be steered from -40^0 to $+40^0$.

Acknowledgment

The authors thank the Scientific and Technological Research Council of Turkey (TÜBİTAK) for their supports under project no 218E039.

References

[1] Zhang S, Huff GH, Feng J, Bernhard JT. A pattern reconfigurable microstrip parasitic array. IEEE Transactions on Antennas and Propagation 2004; 52 (10): 2773–2776. doi: 10.1109/TAP.2004.834372

[2] Chen SL, Qin PY, Lin W, Guo YJ. Pattern-reconfigurable antenna with five switchable beams in elevation plane. IEEE Antennas and Wireless Propagation Letters 2018; 17 (3): 454-457. doi:10.1109/LAWP.2018.2794990

[3] Tran TQ, Sharma SK. Radiation characteristics of a multimode concentric circular microstrip patch antenna by controlling amplitude and phase of modes. IEEE Transactions on Antennas and Propagation 2012; 60 (3): 1601–1605. doi:10.1109/TAP.2011.2180305

[4] Wang Z, Ning Y, Dong Y. Compact Shared Aperture Quasi-Yagi Antenna With Pattern Diversity for 5G-NR Applications. IEE Transactions on Antennas and Propagation 2021; 69 (7): 4178-4183

[5] Zhang GM, Hong JS, Wang BZ, Song G, Li P. Design and time-domain analysis for a novel pattern reconfigurable antenna. IEEE Antennas and Wireless Propagation Letters 2011; 10: 365–368. doi:10.1109/LAWP.2011.2146225

[6] Nguyen-Trong N, Hall L, Fumeaux C. A frequency- and pattern-reconfigurable center shorted microstrip antenna. IEEE Antennas and Wireless Propagation Letters 2016; 15; 1955–1958. doi: 10.1109/LAWP.2016.2544943

[7] Lin W, Wong H, Ziolkowski RW. Circularly polarized antenna with reconfigurable broadside and conical beams facilitated by a mode switchable feed network. IEEE Transections on Antennas and Propagation 2018 66 (2): 996-1001

[8] Jiang X, Zhang Z, Li Y, Feng Z. A novel null scanning antenna using even and odd modes of a shorted patch. IEEE Transactions on Antennas and Propagation 2014; 62 (4); 1903–1909. doi: 10.1109/TAP.2014.2298884

[9] Pal A, Mehta A,Mirshekarr-Syahkal D, Nakano H. A twelve-beam steering low-profile patch antenna with shorting vias for vehicular applications. IEEE Transections on Antennas and Propagation 2017; 68 (8): 3905-3912

[10] Çelik FT, Alatan L, Aydın Çivi Ö. Işıma örüntüsü şekillendirilebilen kompakt mikroşerit yama anten çalışması. In: X. URSI Türkiye 2021 Bilimsel Kongresi; Gebze, Kocaeeli, Türkiye; 2021. (in Turkish)

[11] Balanis CA. Antenna Theory: Analysis and Design. Hoboken, NJ, USA: John Wiley & Sons, 2015.